Depth-resolved measurement of lattice relaxation in $Ga_{1-x}In_xAs/GaAs$ strained layer superlattices by means of grazing-incidence x-ray diffraction

U. Pietsch
Universität Potsdam, FB Physik, Am Neuen Palais 10, D-14415 Potsdam, Germany

H. Metzger and S. Rugel
Universität München, Sektion Physik, Gesch.-Scholl-Platz 1, D-80539 München, Germany

B. Jenichen
Paul-Drude-Institut für Festkörperelektronik, Hausvogteiplatz 5-7, D-10117 Berlin, Germany

I. K. Robinson
AT&T Bell Laboratories, Brookhaven National Laboratory, Upton, New York 11973

(Received 18 August 1992; accepted for publication 2 May 1993)

The state of relaxation in two different superlattices (SLs) of a system with large lattice mismatch, $Ga_{0.8}In_{0.2}As/GaAs$ grown on GaAs [001] by molecular beam epitaxy, has been investigated by surface-sensitive grazing-incidence diffraction (GID). The SL is squeezed between the substrate and a thick GaAs top layer. The thickness of individual GaInAs layers t_a (active layer) is the same in both samples, while the GaAs barrier thickness t_b is different. We have studied the influence of the thickness ratio t_b/t_a on the state of relaxation for different distances from the sample surface. We find that for thick barriers the whole SL remains coherently strained and for the thinner barrier thickness the SL is partially relaxed against the the GaAs top layer. The GID technique was applied for the first time to obtain depth resolution of the lateral lattice parameter in a SL. It is demonstrated to be especially well suited for SL systems with a small difference of the average electron density between the sublayers. The scattering contrast is improved by measuring the intensity as a function of the exit angle ("rod scans") from the "weak" (200) Bragg reflection. Comparing computer simulations with the measured variation of the scattering contrast between GaAs and GaInAs layers obtained from different "information depths" and at different angular positions of the in-plane rocking curves, the state of relaxation can quantitatively be evaluated. On the basis of these results we propose two models for the partial relaxation of the SL into the state of strain-reduced domains. We believe that the partial relaxation is due to the elastic field interaction between the GaInAs layers accross the GaAs barriers, if t_b is small.

03 March 2024 00:33:08

I. INTRODUCTION

Strained layer superlattices (SLs) such as $Ga_{1-x}In_xAs/GaAs$ are characterized by a large lattice parameter difference between both sublayers. Lateral lattice matching is only possible up to a critical thickness t_{cr} beyond which misfit dislocations are created at the interfaces. The understanding of the coherent growth and the evaluation of the mechanism of relaxation are very important for electronic applications. Most of such investigations have been performed using photoluminescence (PL) techniques because a small number of misfit dislocations reduces the PL intensity dramatically. Unfortunately the "information depth" of the PL signal is restricted to some nanometers, which makes it impossible to investigate the whole SL. The progressive state of relaxation can be investigated using conventional x-ray diffraction (XRD), where the lattice mismatch between the SL and substrate in growth direction $\Delta a_\perp /a$ is measured.[1,2] Only averaged parameters can be obtained since the penetration depth of the probing x-ray beam is usually much larger than the total thickness of the SL, t_{tot}. The lateral lattice mismatch $\Delta a_\parallel /a$ cannot be measured directly. In this paper we show that the technique of grazing-incidence x-ray diffraction[3] (GID) yields information on the lattice parameter mismatch as a function of the distance below the sample surface. The "information depth" t_{inf} is controlled by the angles of incidence α_i and exit α_f of the x-ray beam with respect to the sample surface both being close to the critical angle for total external reflection, α_c. The density profile in the growth direction of the SL is probed measuring the intensity distribution along α_f ("rod scan") for different α_i at any lateral Bragg angle Θ_i. This technique was successfully applied to characterize lattice-matched superlattices.[3,4] For partially relaxed SLs one may expect a splitting of the in-plane Bragg peaks which can be probed as a function of depth.

II. EXPERIMENTAL DETAILS

We have investigated two different $(Ga_{1-x}In_xAs/GaAs)_n$ SLs, grown on a GaAs [001] substrate by molecular beam epitaxy (MBE). Their layer sequence is schematically shown in Fig. 1. The samples have almost the same t_{tot}, In content, and t_a but different barrier widths t_b. According to the sample fabrication, both samples are covered by about 300 nm GaAs. The nominal structure parameters of both SLs are given in Table I.

In order to characterize the in-plane lattice parameter $a_\parallel$ as a function of depth and thus the state of relaxation,

 © 1993 American Institute of Physics

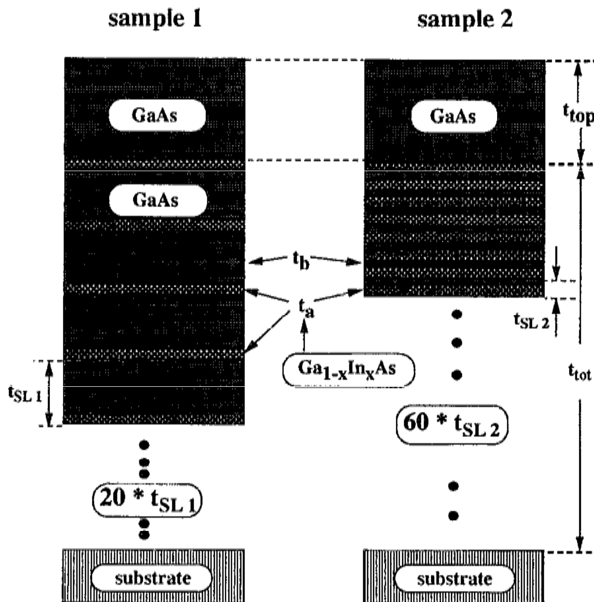

FIG. 1. Schematic view of the layer sequence of the samples used.

GID measurements were performed at the X16A beam line of the National Synchrotron Light Source (NSLS) at Brookhaven National Laboratory. The instrument is described elsewhere.[5] We used a wavelength of $\lambda=0.1749$ nm. The α_i resolution of the incoming x-ray beam and the α_f resolution (position-sensitive detector) were about 0.01°. The GID geometry used is shown in Fig. 2. The incoming beam hits the sample surface under the incident angle α_i. The intensity, I_H, reflected at Θ_B from the lattice planes perpendicular to the surface is measured by a position-sensitive detector (PSD) which resolves the intensity as a function of the exit angle α_f (α_f or rod scan). Comparing rocking curve measurements at different α_i and α_f settings, depth-resolved lattice parameters can be obtained.

III. RESULTS

Rocking curves (RC) of the in-plane (400) and (200) reflections were measured in GID geometry. The peak

TABLE I. Structure parameters of the two samples used. An asterisk indicates values which are obtained from XRD measurements. The GID results which are separated by | correspond to the proposed model 1 and 2, respectively.

	Nominal		GID	
Parameter	Sample 1	Sample 2	Sample 1	Sample 2
t_b (nm)	40	3	42.0±0.5	2.9±0.3
t_a (nm)	13	13	12.5±0.5	12.1±0.2
t_{SL} (nm)	53	16	54.5±1.0	15.0±0.5
t_{top} (nm)	300	300	300	⩽100 | 280±50
n	20	60	20*	60*
In content (%)	24	24	17±2	21*
$\Delta a_\parallel/a$ (10^{-4})			0±5	0–63±5 | 63
t_{relax} (nm)			0	150±30 | 0±50

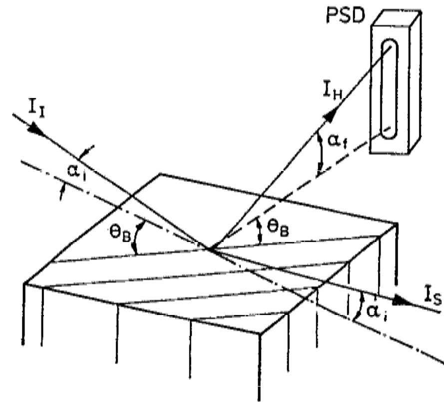

FIG. 2. Scattering geometry for diffraction under grazing incidence and exit angles.

shape of the (400) for sample 1 is Gaussian with a width corresponding to the instrumental resolution ($\Delta\Theta\approx0.02°$). The (400) peak width of sample 2 is about 8 times broader [Fig. 3(a)] and shows a very weak shoulder at its low angle side (position 3). It indicates the existence of a small vol-

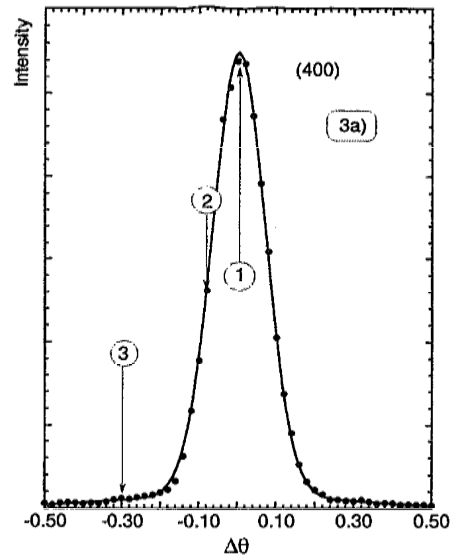

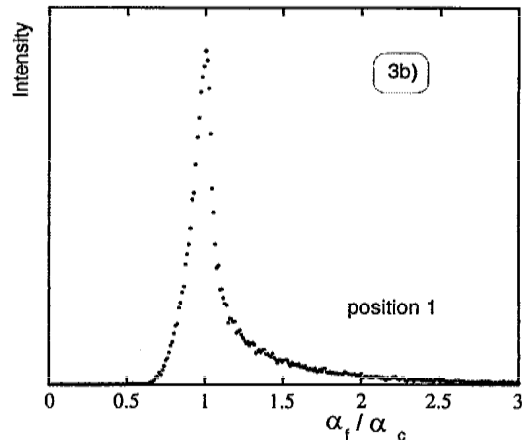

FIG. 3. (a) In-plane (400) rocking curve and (b) α_f-resolved rod scan measured from sample 2 at position 1 for $\alpha_i=0.8°\approx2.8\alpha_c$.

03 March 2024 00:33:08

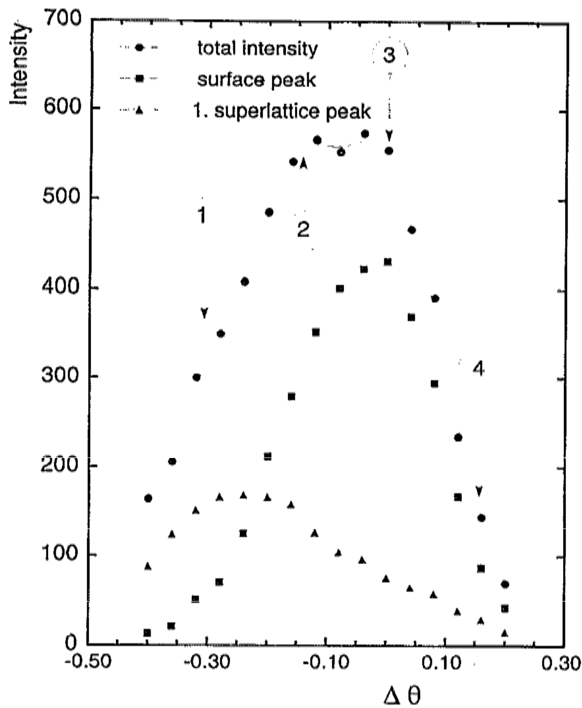

FIG. 4. In-plane (200) rocking curve of sample 2 (circles). The squares and triangles indicate curves which are recorded for the strained and the relaxed component of SL separately.

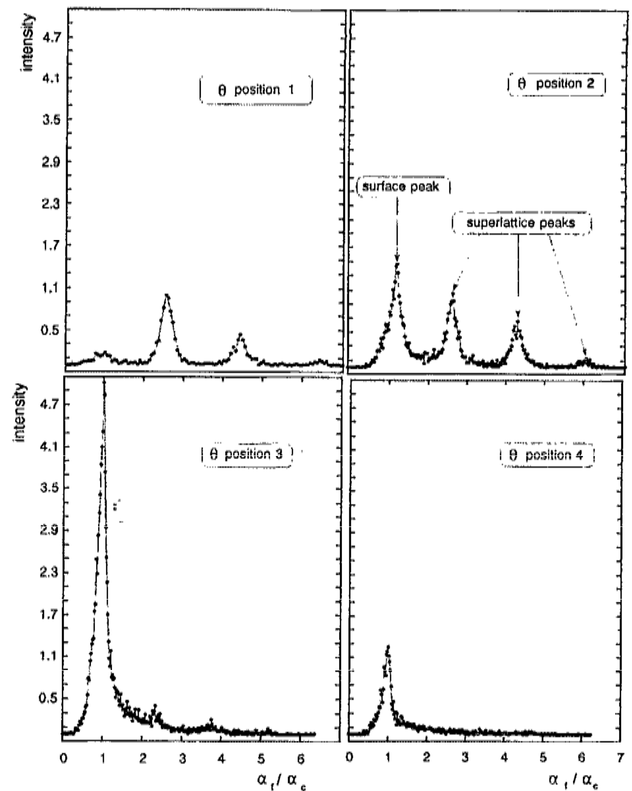

FIG. 5. α_f rod scans measured at the (200) rocking curve of sample 2 at the four Θ_i positions marked in Fig. 4.

ume fraction with a distribution of lattice parameters within the information depth. The α_f scans at positions 1 and 2 exhibit the typical shape of a surface peak with a maximum for $\alpha_f=\alpha_c$ [see Fig. 3(b), for example]. They do not show any modulation for $\alpha_f>\alpha_c$, which would demonstrate the layered sequence of the SL in the growth direction. This can be explained by the very small difference in the scattering power between the sublayers (see later).

In contrast, the features are quite different for the weak reflection (200). Sample 1 still shows only one symmetrical peak, again with the width determined by the instrumental resolution ($\Delta\Theta\approx0.02°$). For sample 2 the RC of the (200) at $\alpha_i=0.7°\approx2.5\alpha_c$ is shown in Fig. 4. The Bragg intensity integrated over α_f (filled circles) is given as a function of $\Delta\Theta$. The RC is asymmetric around the angular position of the unstrained GaAs (200) reflection ($\Delta\Theta=0°$). The width has increased by about 10 times the instrumental resolution. The origin of the asymmetry given by the sum of two other curves in Fig. 4 (squares and triangles) becomes clear by first investigating the α_f-resolved Bragg intensity distribution shown in Fig. 5. These distributions measured at $\alpha_i=0.7°$ are given at four in-plane Θ_i positions indicated by the number i and arrows in the previous Fig. 4. Figure 5 will be explained in detail: At position 4, only the surface peak is visible. At position 1 the surface peak has almost vanished and only SL peaks remain. Thus the "surface peak" at $\alpha_f=\alpha_c$ and the SL peaks at $\alpha_f>\alpha_c$ have their maxima at different Θ positions. The Θ dependence of the surface peak is given by squares in Fig. 4 while the corresponding distribution of the SL peaks is marked by triangles. Figure 4 clearly demonstrates that the total Bragg intensity originates from the sample with a depth-dependent distribution of lattice parameters. This distribution is quantitatively obtained from a detailed investigation of the intensities in Fig. 5 (see discussion and Fig. 6). Qualitatively Fig. 5 can be interpreted as follows: Θ_3 marks the Bragg position of the unstrained GaAs top layer. At Θ_1 only the relaxed part of the structure fulfills the Bragg condition. Since the surface peak measures primarily the GaAs overlayer and the SL peaks give information on the strained SL regions, the corresponding RCs can be evaluated separately. The peak splitting $\Delta\Theta$ in Fig. 4 (squares and triangles) is interpreted in terms of the inplane lattice mismatch $\Delta a_{\|}/a=-\Delta\Theta\tan\Theta_B$. In order to investigate this mismatch as a function of the depth from the sample surface, measurements like those in Figs. 4 and 5 have been performed for different angles of incidence α_i. The results are shown in Fig. 6 where the mismatch $\Delta a_{\|}/a$ measured with respect to the GaAs top layer is given as a function of α_i on the lower horizontal scale. More important is the upper scale where the corresponding information depth t_{inf} is noted, as calculated from Eq. (6) below. Near the surface ($\alpha_i<\alpha_c$) only the GaAs top layer is measured, therefore $\Delta a_{\|}/a$ is approximately zero. The lattice parameter increases with the penetration depth of the probing x ray to a mismatch value of $\Delta a_{\|}/a=+(6.3\pm0.5)\times10^{-3}$ measured in a depth of about 300 nm. This mismatch amounts to about 40% of the expected value for GaInAs after a complete relaxation into the cubic state ($\Delta a_{\|}^{\max}/a=0.0153$). The evaluated

03 March 2024 00:33:08

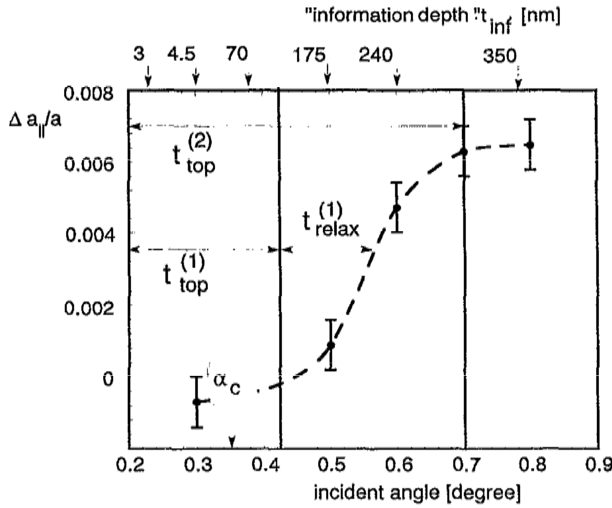

FIG. 6. Variation of the in-plane lattice mismatch $\Delta a_{\|}/a$ as a function of α_i (e.g., information depth, t_{inf}) evaluated from the peak splitting between the strained (squares) and relaxed (triangles) SL component as shown in Fig. 4. $t^{(1)}_{top}$ and $t^{(1)}_{relax}$ correspond to the fitted values of model 1 and $t^{(2)}_{top}$ to model 2.

parameters shown in Table I were obtained via simulation of the α_f-resolved Bragg intensity measured at different α_i.[3]

IV. INTERPRETATION

For the present case of a weak reflection and imperfect (relaxed) SL the kinematical scattering theory can be applied to explain the GID curves.[6,7] In this approach the total scattering intensity is given by[8,9]

$$I(\alpha_f) \approx \exp(-\sigma^2 k_0 q)[T(\alpha_i)S(q)T(\alpha_f)]^2, \quad (1)$$

which contains Fresnel's transmission functions T with respect to α_i and α_f and an overall damping function with the parameter σ for surface and interface roughnesses. In the present case $T(\alpha_{i,f})$ are calculated taking into account an average density of the SL. The periodicity in growth direction is expressed by the structure amplitude $S(q)$,

$$S(q) = \int dz\, X_H(z)\exp(iq_z z), \quad (2)$$

which depends on the scattering vector

$$q = |k_f - k_i| = k_0(\sqrt{\alpha_i^2 + \langle X_0\rangle} + \sqrt{\alpha_f^2 + \langle X_0\rangle}) \quad (3)$$

with $k_0 = 2\pi/\lambda$. X_0 and X_H stand for the dielectric susceptibility at $q=0$ and reciprocal-lattice vector H. $\langle X_0\rangle$ is average over the whole SL. This is justified by the small difference in X_0 between the sublayers. The shape of the intensity distribution versus α_f is determined mainly by T resulting in a peak at $\alpha_f = \alpha_c$ ("surface peak").[10] For higher α_f SL peaks appear for $\alpha_f = \alpha_s$. In case of $\alpha_f > 2\alpha_c$ the angular separation $\Delta\alpha_S$ is a measure for t_{SL}

$$\Delta\alpha_s = \lambda/t_{SL}. \quad (4)$$

We find $t_{SL} = 54.3 \pm 0.3$ and 15.0 ± 0.4 nm for samples 1 and 2, respectively. The intensity of the SL peaks is controlled by $S(q)$. The scattering contrast depends on the difference in the electron density X_0 and in the scattering power X_H between the two sublayers. X_0 and X_{400} differ by approximately 1% only between GaAs and $Ga_{0.8}In_{0.2}As$ (Table II). This explains the missing SL peaks in Fig. 3. Only the "weak" (200) reflection allows an enhancement of the scattering contrast, because X_{200} depends on the difference in the electron density between both fcc sublattices of the zinc-blende structure. For $Ga_{1-x}In_xAs$, $|X_{200}|$ vanishes at $x \approx 0.1$ and is about 30% larger than that for GaAs at $x = 0.21$. The varying contrast in the (200) α_f-resolved scans at the different Θ_i positions of sample 2 (Fig. 5) is due to the different Θ dependence of the scattering powers of the GaAs top layer and the relaxed SL. At Θ_3 the RC is dominated by the scattering power of the top layer and the eventually unrelaxed part of the SL, whereas the relaxed part of the structure contributes only with about 15%–20% of the maximum value of the total intensity. Their contribution is further reduced by the absorption in the top layer. On the other hand, the relaxed part scatters predominantly at Θ_1 (triangles in Fig. 4), whereas the scattering power of the top layer is reduced due to the different angular position of the GaAs in-plane RC (squares in Fig. 4).

TABLE II. Real and imaginary parts of scattering coefficients $X_{0,H}$ used for simulating the GID α_f scans, given in units of 10^{-6}.

	GaAs	$Ga_{0.8}In_{0.2}As$
$Re(X_0)$	37.8	38.8
$Im(X_0)$	1.4	2.1
$Re(X_{400})$	21.8	22.0
$Im(X_{400})$	1.30	1.78
$Re(X_{200})$	1.01	1.06
$Im(X_{200})$	0.15	0.90

V. MODEL CALCULATIONS

Two models of relaxation are proposed in order to interpret our results.

Model 1: If only the GaInAs layers relax against the lattice parameter of the GaAs top layer and the GaAs barriers, the evaluated variation of $\Delta a_{\|}/a$ with depth (Fig. 6) at any fixed Θ_i may be approximated by the scattering power $X_{200}(t)$:

$$X_{200}(t) = \begin{cases} X_{200}(\Theta)*(c/2)\{\tanh[(t-t_{relax})/t_{tot}]+1\} \\ \quad \text{for } Ga_{0.8}In_{0.2}As \\ X_{200}^{layer}(\Theta) = X_{200}^{top}(\Theta) = \text{const} \quad \text{for GaAs}. \end{cases} \quad (5)$$

The strain profile of the GaInAs layers is simulated by a simple numerical function depending on two parameters: the depth for which the relaxation reaches its half maximum t_{relax} and a parameter c describing the slope at t_{relax}. At any Θ_i the changing α_f contrast measured for different α_i is related to different information depths,[10]

$$t_{inf} = k_0[\mathrm{Im}(\sqrt{\alpha_i^2 + \langle X_0\rangle}) + \mathrm{Im}(\sqrt{\alpha_f^2 + \langle X_0\rangle})]^{-1} \quad (6)$$

03 March 2024 00:33:08

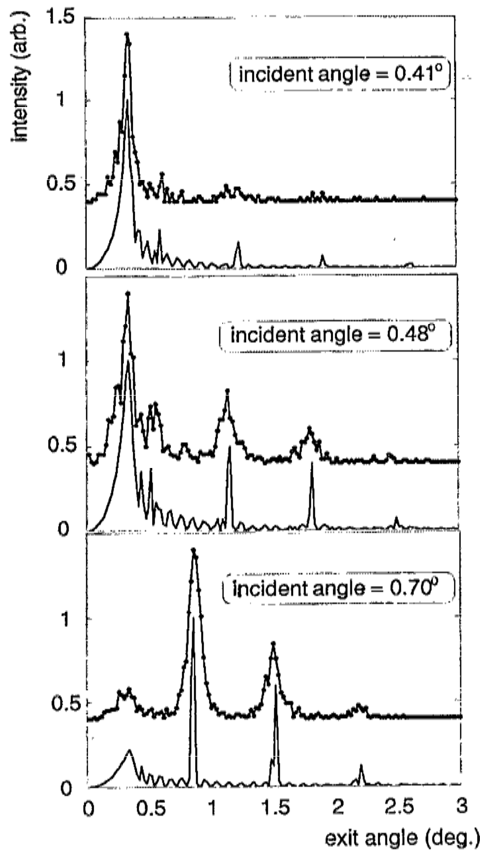

FIG. 7. Comparison between measured and simulated α_f-resolved curves at three different α_i positions for sample 2 and at the Θ position 1 of Fig. 4.

and can be simulated by two relevant parameters, t_{relax} and $X_{200}(\Theta)$. Their values are modified by $x(\text{In})$ and t_{top}.

The results of the fitting procedure for the α_f scans at different α_i in the Θ_1 position of Figs. 4 and 5 is shown in Fig. 7. The SL peak positions and the changing contrast are correctly described by our model calculation. In order to reduce the number of parameters the In content of the active layer was taken from the lattice mismatch between the sublayers as measured by conventional x-ray diffraction.[11] It corresponds to $x(\text{In})=0.19\pm0.01$ and 0.21 ± 0.01 for samples 1 and 2, respectively. The α_f distribution of the intensity turns out to be very sensitive to t_{top} and t_{relax}, which are interdependent, however. Best fitting results are obtained for $t_{top}<100$ nm and $t_{relax}\approx150$ nm. Thus we conclude that the SL remains strained up to about 10 SL periods below the GaAs top layer. However, the fitted t_{top} is quite different from its nominal value of 300 nm.

Model 2: In this model the in-plane lattice parameter of the GaAs barriers are assumed to coincide with that of the sandwiched and partially relaxed GaInAs layers while the GaAs top layer retains its intrinsic lattice parameter. The scattering power of the investigated part of the SL is nearly independent of depth. The scattering contrast as a function of Θ is only due to the lattice parameter difference between the top layer and the SL. Using $x(\text{In})=0.21$ we obtain $t_{top}\approx280\pm50$ nm and $t_{relax}\approx0\pm50$ nm from corresponding simulations. In this model the relaxed region of the SL begins directly below the GaAs top layer accompanied by a region of large lattice distortion in the GaAs top layer near the interface to the relaxed SL. The corresponding fits of the α_f scans for model 2 are the same as those for model 2 as given in Fig. 7. Unfortunately the interface region cannot be resolved better because the thickness of the top layer is close to the maximum information depth. Thus the α_f simulation for models 1 and 2 give the same results. From our GID measurements alone it seems impossible to distinguish between one of the two models. Model 2 results in a better agreement with the nominal value for t_{top} and the peak shape of the (400) RC of sample 2 can be explained more easily by model 2. Caused by the nearly identical scattering power of the top layer and the relaxed SL and the large distance of the SL below the surface, the contribution of the relaxed region to the RC at (400) is much smaller than that for the (200) reflection. Thus the (400) RC depends primarily on the GaAs top layer, and its large peak width is due to the high defect density caused by the incoherent growth on the relaxed support.

On the other hand, the large widths of the (200) RC as well as the width of the α_f-resolved SL peaks for sample 2 (Figs. 4 and 7) are primarily a measure for the real structure within the SL. Using plane-wave topography a high density of misfit dislocations was obtained.[12] They induce partial relaxation, resulting in microcrystalline domains, which can be macroscopically measured by an orientational distribution of diffracting lattice planes and a lateral fluctuation of their thicknesses t_{SL} within the SL. Assuming that the widths $\Delta\Theta_{in}$ and $\Delta\alpha_f$ are primarily caused by the size $t_{lateral}$ and $t_{vertical}$ of these domains, we obtain a rough estimate using the Scherrer equation[12]

$$t_{lateral}\approx\lambda/(\Delta\Theta_{in}\cos\Theta_{in}),\quad t_{vertical}\approx\lambda/(\Delta\alpha_f\cos\alpha_f). \tag{7}$$

From the half width of the measured SL peaks $\Delta\alpha_f\approx0.15°$ we find $t_{vertical}\approx63\pm10$ nm. This corresponds to a domain height of about $n\approx4$ or 5 SL cells. In order to approximate the lateral size we use the measured width of the (200) RC (squares in Fig. 4) reduced by the experimental resolution. We find $t_{lateral}\approx70\pm10$ nm in close agreement to $t_{vertical}$. The obtained domain size evaluated in the growth direction from the GID is compatible to those obtained from the width of the SL peaks measured by conventional x-ray diffraction.[11] From the corresponding curves for sample 1 (not shown here) we find $t_{vertical}>150$ nm and $t_{lateral}>500$ nm as an upper limit for a possible domain size as obtained from the fact that the peak width is given by the instrumental resolution.

VI. DISCUSSION

Our results can be interpreted by the following model of lattice relaxation. The thickness of an individual $Ga_{0.8}In_{0.2}As$ layer within the SL is much smaller than t_{cr} of a single $Ga_{0.8}In_{0.2}As$ layer on GaAs, which amounts to about 19 nm.[2,13] During growth and cooling, the GaInAs layers become more and more strained. Their strain fields

03 March 2024 00:33:08

interact across the GaAs barriers, if t_b is small. Thus the GaInAs layers are no longer isolated. In this case the critical thickness for relaxation of the SL includes some SL periods, $t_{cr}^{SL}=n_{cr}t_{cr}$. This condition is obviously given for sample 2 but not for sample 1. $t_{cr}^{SL}\approx t_{cr}$ holds in the case of strain isolated layers like sample 1. In sample 2 the relaxation process may begin in the middle of the SL. If t_{cr}^{SL} is reached, misfit dislocations are induced primarily at each n_{cr}th interface. Thus relaxation takes place in domains separated from each other by misfit dislocations. The degree of relaxation may be different from one domain to the other, which results in a distribution of the in-plane lattice parameter.

n_{cr} can roughly be estimated by the following strain model: Let V_{cr} be the strain energy of a single strain isolated GaInAs layer grown on a thick unstrained GaAs substrate. Assuming that the domains have the shape of columns with dimension a^2t (a^2 is the basal plane and t the length perpendicular to the growth direction), then $V=V_{cr}$ defines the strain energy at $t=t_{cr}$,

$$V_{cr}=t_{cr}a^2K\epsilon^2. \tag{8}$$

K stands for the elastic constant, which depends on the strain direction, and ϵ is the maximum strain of the layer, which amounts to $\epsilon_{max}=\Delta a_{\parallel}^{max}/a=0.0153$ in the case of a lattice-matched strained $Ga_{0.8}In_{0.2}As$ on GaAs[001]. Assuming the same strain energy can be deposited within relaxed SL domains containing GaInAs and GaAs layers with the same lateral lattice parameter $a_{\parallel}$, we can determine n_{cr} from

$$V_{cr}^{SL}/a^2K=V_{cr}/a^2K=n_{cr}(t_b\epsilon_{GaAs}^2+t_a\epsilon_{GaInAs}^2), \tag{9}$$

using $K\approx K_{GaAs}\approx K_{GaInAs}$ and assuming linear superposition of strain in the two sublayers. The right-hand side contains the strain of the GaAs layers measured with respect to the unstrained substrate $\epsilon_{GaAs}=(\Delta a_{\parallel}^{expt}/a)$ and the released strain of the GaInAs layers $\epsilon_{GaInAs}=\epsilon_{max}-(\Delta a_{\parallel}^{expt}/a)$. Using the respective values for sample 2 (Table I) we find $n_{cr}=4.2$, resulting in $n_{cr}(t_a+t_b)\approx 63$ nm. This is in agreement with the experimental results. For sample 1 and using $\Delta a_{\parallel}^{expt}/a<10^{-4}$ we find $n_{cr}\approx 1.4$, which documents the situation of strain isolation of the GaInAs layers. In this case the critical thickness t_{cr} of a single layer is approximately equal to t_{cr}^{SL}.

The relaxation process of the SL ends near the thick top layer and the substrate, respectively, for models 1 and 2. The interfaces may undergo a grading of relaxation within the SL (model 1) or a constant relaxation over the whole SL with a grading of the lattice parameter within the GaAs in order to compensate the lattice mismatch to the relaxed support (model 2). This situation seems reasonable for the top layer of sample 2. In fact Krol *et al.*[14] have found by electron microscopy studies macroscopically strained and unstrained regions which may indeed coexist together. Model 2 is further supported by recently performed measurements.[15] For samples nearly identical to those used in this work but without a top layer we found a constant relaxation beginning from the surface up to the maximum information depth of the x rays.

Model 1 should describe the state of relaxation near the interface between the SL and the substrate for which the SL has to compensate the lattice mismatch with respect to GaAs. Unfortunately, this interface could not be investigated since the total thickness of the SL plus top layer is way beyond the information depth of our GID experiment.

VII. CONCLUSIONS

Our measurements show that sample 1 is macroscopically fully strained. Caused by the large barrier thickness t_b an elastic interaction across the barriers is not possible and thus the GaInAs layers remain strained, isolated from each other by the thick GaAs barrier layers. The measured half widths of the SL reflections in the α_f-resolved GID are smaller than those for sample 2 but larger than those expected for a perfect crystal. This may indicate the presence of misfit dislocations, which were in fact observed by plane-wave topography[11] but which do not lead to complete relaxation.

Samples 1 and 2 may represent two different states of relaxation, the initial and a progressed state, respectively. Our results are in agreement with Hovinen, Salokatve, and Asonen[16] and Grey *et al.*,[17] who have shown by means of PL measurements that macroscopic relaxation appears for $t_b/t_a<1$. Further experiments are necessary in order to define the crossover thickness ratio t_b/t_a which is necessary for elastic isolation of strained layers.

From the experimental point of view we presented GID measurements to characterize the state of relaxation and the real structure of two SLs with lattice mismatch as a function of depth. By means of the Θ_i- and α_f-dependent variation of the scattering contrast, the depth below the surface in which the relaxation occurs was evaluated. Although the sensitivity of GID measurements is unique with respect to $\Delta a_{\parallel}/a$ and its depth resolution, complimentary conventional x-ray diffraction (rocking curves) are desireable in order to reduce the number of fit parameters.

ACKNOWLEDGMENTS

This work was supported by BMFT Grants (No. 05 5IPAAI 8, No. 03 PE2LMU 0, and No. 05 5WMAXI). The authors thank Dr. P. Claxton for supplying the samples. One of us (U.P.) thanks the Alexander-von-Humboldt Foundation and Professor J. Peisl for their generous promotion.

[1] R. Flagmeyer, U. Pietsch, H. Rhan, M. Möricke, and B. Jenichen, Phys. Status Solidi A **113**, 211 (1989).

[2] P. J. Orders and B. F. Usher Appl. Phys. Lett. **50**, 980 (1987).

[3] U. Pietsch, W. Seifert, J.-O. Fornell, H. Rhan, H. Metzger, S. Rugel, and J. Peisl, Appl. Surf. Sci. **54**, 502 (1992).

[4] U. Pietsch, in *Surface X-Ray and Neutron Scattering*, edited by H. Zabel and I. K. Robinson, Proceedings in Physics (Springer, Berlin, 1992), Vol. 61, p. 223.

[5] P. O. Fuoss and I. K. Robinson, Nucl. Instrum. Methods **222**, 171 (1984).

[6] H. Rhan, U. Pietsch, H. Metzger, S. Rugel, and J. Peisl, J. Appl. Phys. **74**, 146 (1993).

[7] U. Pietsch, H. Rhan, A. L. Golovin, and Yu. Dmitriev, Semicond. Sci. Technol. **6**, 743 (1991).

03 March 2024 00:33:08

[8] G. D. Vineyard, Phys. Rev. B **26**, 4146 (1982).
[9] S. K. Sinha, E. B. Sirota, S. Garoff, and H. B. Stanley, Phys. Rev. B **38**, 2297 (1988).
[10] H. Dosch, B. Battermann, and D. C. Wuck, Phys. Rev. Lett. **56**, 1144 (1986).
[11] B. Jenichen and R. Köhler, *Proceedings of the MRS Fall Meeting*, Boston, 1992, edited by D. C. Houton, C. W. Tu, and R. T. Tung (MRS, Pittsburgh, PA).
[12] H. P. Klug and L. E. Alexander, *X-Ray Diffraction Procedures*, 2nd ed. (Wiley, New York, 1974).
[13] J. W. Matthews and A. E. Blakeslee, J. Cryst. Growth **27**, 118 (1974).
[14] A. Krol, H. Resat, C. J. Sher, S. C. Woronick, W. Ng, Y. H. Kao, T. L. Cole, A. K. Green, C. K. Lowe-Ma, T. W. Nee, and V. Rehn, J. Appl. Phys. **69**, 949 (1991).
[15] D. Rose, U. Pietsch, A. Förster, and H. Metzger, Proceedings of the 3rd International Conference on Surface X-ray and Neutron Scattering, Dubna, Russia, 1993 (to be published).
[16] M. Hovinen, A. Salokatve, and H. Asonen, J. Appl. Phys. **69**, 3378 (1991).
[17] R. Grey, J. P. R. David, P. A. Claxton, F. Gonzales Sanz, and J. Woodhead, J. Appl. Phys. **66**, 975 (1989).

03 March 2024 00:33:08